Pergamon

Neuropharmacology 42 (2002) 306–318

NEURO PHARMACOLOGY

www.elsevier.com/locate/neuropharm

Functional expression of distinct NMDA channel subunits tagged with green fluorescent protein in hippocampal neurons in culture

J.-H. Luo[a], Z.-Y. Fu[a], G. Losi[a], B.G. Kim[a], K. Prybylowski[a], B. Vissel[b], S. Vicini[a,*]

[a] *Department of Physiology and Biophysics, Georgetown University School of Medicine, 3900 Reservoir Road NW, Washington, DC, 20007, USA*

[b] *Molecular and Neurobiology Laboratory, Salk Institute, La Jolla, CA, USA*

Received 13 September 2001; received in revised form 21 November 2001; accepted 28 November 2001

Abstract

We generated expression vectors for N-terminally green fluorescent protein -tagged NR2A and NR2B subunits (GFP-NR2A and GFP-NR2B). Both constructs expressed GFP and formed functional NMDA channels with similar properties to untagged controls when co-transfected with NR1 subunit partner in HEK293 cells. Primary cultured hippocampal neurons were transfected at five days in vitro with these vectors. Fifteen days after transfection, well-defined GFP clusters were observed for both GFP-NR2A and GFP-NR2B subunits being co-localized with endogenous NR1 subunit. Whole-cell recordings showed that the GFP-NR2A subunit determined the decay of NMDA-mediated miniature spontaneous excitatory postsynaptic currents (NMDA-mEPSCs) in transfected neurons. Live staining with anti-GFP antibody demonstrated the surface expression of GFP-NR2A and GFP-NR2B subunits that was partly co-localized a presynaptic marker. Localization of NMDA receptor clusters in dendrites was studied by co-transfection of CFP-actin and GFP-NR2 subunits followed by anti-GFP surface staining. Within one week after plating most surface NMDAR clusters were distributed on dendritic shafts. Later in development, a large portion of surface clusters for both GFP-NR2A and GFP-NR2B subunits were clearly localized at dendritic spines. Our report provides the basis for studies of NMDA receptor location together with dendritic dynamics in living neurons during synaptogenesis in vitro. © 2002 Published by Elsevier Science Ltd.

Keywords: NMDA receptors; Green fluorescent protein; Excitatory postsynaptic current; Development

1. Introduction

A crucial step in synaptic development and plasticity is the clustering, targeting and accumulation of receptors at the postsynaptic site. In excitatory hippocampal synapses, N-methyl-D-aspartate (NMDA) receptors are expressed before AMPA receptors and are required for activity-dependent rearrangements of synapses during CNS development (Sheetz and Constantine-Paton, 1994). Three gene families (NR1, NR2 and NR3) that encode NMDA receptor subunits have been identified (Dingledine et al., 1999; Cull-Candy et al., 2001 for review). The NR2 genes encode four subunits named NR2A, NR2B, NR2C and NR2D. Different NR2 subunits have specific developmental expression profiles and endow the NMDA receptor with distinct channel properties, and the predominantly expressed NR2 subunits in hippocampus and neocortex are NR2A and NR2B (Cull-Candy et al., 2001).

The relative contribution of NR2A and NR2B subunits to native NMDA receptor channel varies developmentally with functional consequences (Cull-Candy et al., 2001). A change in functional properties of the NMDA receptors has been proposed as a potential mechanism contributing to the loss of synaptic plasticity during brain maturation (Daw et al., 1993; Sheetz and Constantine-Patton, 1994; Fox et al., 1999 for review). Thus, it is important to understand the structural and functional diversity of NMDA receptors in relationship to NMDA receptor subunit composition and spatial distribution at excitatory synaptic sites during development.

Receptor protein dynamics in living cells can be studied with fluorescent microscopy, photobleaching and resonance energy transfer by taking advantage of tagging receptor subunit proteins with a fluorescent protein. To

* Corresponding author. Tel.: +1-202-687-6441; fax: +1-202-687-7407.

E-mail address: svicin01@georgetown.edu (S. Vicini).

0028-3908/02/$ - see front matter © 2002 Published by Elsevier Science Ltd.
PII: S0028-3908(01)00188-5

this aim, the green fluorescent protein (GFP) from the jellyfish *Aequorea victoria* is an ideal tool. Indeed, GFP-tagged proteins, both in the cytosol and in the plasma membrane, have been studied (Cubitt et al., 1995, 1999 for review). To study the localization, distribution and dynamics of neurotransmitter receptors, however, an essential condition is that GFP tagging does not alter binding or functional properties of the receptor. Ligand-gated channel subunits tagged with GFP in transfected neurons have been used for studies of $GABA_A$, glycine and AMPA receptors (Connor et al., 1998; David-Watine et al., 1999; Shi et al., 1999). A GFP-tagged version of the NMDA receptor subunit NR1 (Marshall et al., 1995) has been transfected in mammalian HEK293 cells and demonstrated to produce functional NMDA receptors when co-transfected with NR2A subunit. More recently, the NR1 subunit tagged at the C terminus with GFP has been shown to form fluorescent clusters in transfected cultured hippocampal neurons (Crump et al., 2001).

Preparations of cultured neurons have several advantages for the study of receptor distribution and synapse formation. Indeed, the occurrence of highly motile dendritic filopodia as precursors of synapse formation was reported first for neurons in culture (Dailey and Smith, 1996; Ziv and Smith, 1996; Fisher et al., 1998) and later demonstrated to occur in vivo (Maletic-Savatic et al., 1999; Lendvai et al., 2000). At the same time, immunocytochemical studies of the distribution of NMDA receptor subunits in primary cultured neurons showed evidence for a developmental increase of NR2A subunit-containing receptor clusters, particularly at synaptic sites (Li et al., 1998). In this study, we investigate the expression and distribution of the NR2A and NR2B NMDA receptor subunits in primary cultured hippocampal neurons transfected with GFP-tagged NMDA receptor subunits and stained with specific antibodies. In parallel, we report specific alterations of NMDA receptor-mediated spontaneous synaptic currents resulting from the selective expression of GFP-tagged subunits at excitatory synapses in these neurons. Last, we describe the localization of GFP-tagged NR2 subunit clusters with respect to a presynaptic marker and to dendritic structures at the time of synaptogenesis.

2. Materials and methods

2.1. GFP-tagged NR2 subunits and CFP–actin constructs

The expressional vector for GFP-NR2B has been constructed by inserting a GFP cDNA fragment in frame with the NR2B subunit between the fifth and sixth codons after the predicted sequence for signal peptide. In GFP-NR2A, GFP was inserted between the fifteenth and sixteenth codons. cDNA encoding GFP was amplified by polymerase chain reaction (PCR) from plasmid pEGFP (Clontech, Palo Alto, CA). The construct for cyan fluorescent protein-tagged actin at the N terminus (CFP-actin) was generated by replacing the GFP sequence of pEGFP-actin (Clontech) with CFP fragment of pECFP-N1 (Clontech) between *Nhe*I and *Bsr*GI sites.

2.2. Primary hippocampal neuronal cultures and transfections

Hippocampal neuronal cultures were prepared from one-day-old Sprague Dawley rats. Briefly, after careful dissection from diencephalic structures, the hippocampi were chopped and digested in 0.28% trypsin (Sigma, St Louis, MO) for 15 min at 37 °C with gentle shaking. Dissociated cells were plated at a density of 2×10^6 in a 35-mm dish with poly-L-lysine coated coverslips in Basal Eagle Medium (BME, Invitrogen, Carlsbad, CA) containing 10% FBS, 2 mM glutamine, 100 μg/ml gentamycin (all from Invitrogen Corporation Carlsbad, CA), and 25mM KCl, and maintained at 37 °C in 5% CO_2. After 24 hours in vitro, the medium was replaced with a half and half mixture of BME and Neurobasal medium containing 2% B27 supplement, 1% antibiotic, and 0.25% glutamine (Invitrogen). At five days in vitro (DIV5), cytosine arabinofuranoside was added at a final concentration of 10 μM. Thereafter, half of the medium was replaced twice a week with Neurobasal medium containing 2% B27 supplement, 1% antibiotic, and 0.25% glutamine. Cells were plated on coverslips for immunocytochemistry and physiological recordings. HEK293 cells were transfected with NR1-1a and GFP-NR2A or GFP-NR2B using calcium phosphate precipitation (Chen and Okayama, 1987). For neuronal transfection the method was slightly modified. Briefly, cultured hippocampal neurons at DIV5 on coverslips were transferred to a well in a 4-well plate with 500 μl transfection medium, a MEM medium (Cat #12370-037, Invitrogen) with adjusted pH to 7.85 by 5M NaOH. Then 30 μl DNA/Ca^{2+} mixture containing 3 μg total cDNA was added and incubated for 30 min at room temperature. After washing with transfection medium, original culture medium was returned and neurons were maintained at 37 <C in 5% CO_2.

2.3. Immunoblotting and immunocytochemistry

Immunoblotting was done as previously described (Luo et al., 1997). Briefly, membranes were prepared from HEK293 cells transfected with cDNAs encoding GFP-tagged NR2A and NR2B. The proteins were solubilized and run on 7.5% SDS-PAGE gels under reducing conditions. Standard Western blot procedure was followed to transfer proteins onto nitrocellulose membranes, incubate with primary antibodies against NR2A

and NR2B (Chemicon, Temecula, CA), and incubate with secondary horseradish peroxidase-conjugated donkey anti-rabbit antibody (Amersham, Arlington Heights, IL). Proteins were visualized with enhanced chemiluminescence (Pierce). Cultured hippocampal neurons were fixed in methanol for 10 min at –20 <C and permeabilized in 0.25% Triton X-100 for 1 min at room temperature. Cells were preincubated in 10% BSA (Sigma) for 1 h at room temperature and then incubated in primary antibodies in phosphate-buffered saline (PBS) containing 3% BSA overnight at 4 °C. A monoclonal antibody against all splice isoforms of the NR1 subunit (Luo et al., 1997) and anti-synaptophysin monoclonal antibody (Chemicon) were used at 1 μg/ml. Rabbit polyclonal anti-NR2B and NR2A subunits (Chemicon) were used at 1:400. After washing with PBS several times, cells were incubated with secondary antibodies for 1 h at room temperature. Both indocarbocyanine (Cy3) secondary antibodies (Jackson ImmunoResearch Laboratories, West Grove, PA) and Alexa-488 conjugated secondary antibodies (Molecular Probes, Eugene, OR) were used at 1:2000. Coverslips were mounted on slides using AntiFade component A (Molecular Probes) as mounting medium.

2.4. Surface staining of living cells and image analysis

Cultured hippocampal neurons were transfected with GFP-NR2A or GFP-NR2B, and sometimes co-transfected with CFP-actin at five days in vitro (DIV). Coverslips were rinsed with extracellular medium (ECM, the same medium used in whole-cell recordings detailed below) and incubated with rabbit polyclonal antibody against GFP (Chemicon) at 2 μg/ml in ECM for 7 min at room temperature. After three washes with ECM, neurons were incubated with Cy3-conjugated goat anti-rabbit antibody (Jackson ImmunoResearch Laboratories) at 1:400 in ECM for another 7 min at room temperature followed by three washes in ECM. Cultures were maintained in a recording chamber in extracellular solution and continuously perfused. Nikon band pass filter cubes were used for GFP and CFP, and the G2A cube was used for Cy3 fluorescence. Living neurons transfected with GFP-NR2A and GFP-NR2B and surface immunostained were imaged on a Nikon EN600 microscope equipped with a 60 x, 1.0 N.A. objective. Digital images were acquired with a Grayscale Microscopy System (RS170, Scion Corporation, Frederick, MD) capturing 10–600 ms exposures. A single level of focus was maintained throughout each recording. Recording at a single focal plane was usually sufficient to capture NMDA receptor clusters throughout the full thickness of small distal dendrites but not of proximal dendrites or cell body. Thus, for our measurements, we estimated the number of clusters only in distal dendrites. Morphometric measurements were performed using MetaMorph image analysis software (Universal Imaging Corporation, Downingtown, PA). Several neurons from two to three coverslips per culture were randomly selected on the basis of healthy morphology and scored to determine the percentage of clusters in segments of dendrites of at least 50 μm length. CCD images were background subtracted, and to define clusters a single threshold was chosen manually so that clusters corresponded to puncta of at least twofold greater intensity than the diffuse fluorescence on the dendritic shaft. NR2 clusters were considered matched when they shared more than half of their pixels. Synaptophysin bouton matching was considered if within 2 pixels from receptor puncta. The weak GFP fluorescence from tagged subunits in permeabilized cells was not detected at the low exposures used in detecting synaptophysin staining. Spines and filopodia were manually traced and measured in several segments of dendrites of at least 50 μm in length.

2.5. Electrophysiology

Transfected HEK-293 cells or hippocampal neurons were voltage-clamped at room temperature. The recording chamber was continuously perfused at 5 ml/min with an extracellular medium (ECM) composed of (in mM): 145 NaCl, 5 KCl, 2 $CaCl_2$, 5 glucose, 0.01 glycine and 5 HEPES at pH 7.4 with NaOH. Osmolarity was adjusted to 325 mOsms with sucrose. Electrodes were pulled in two stages on a vertical pipette puller from borosilicate glass capillaries (Wiretrol II, Drummond). Typical pipette resistance was 5 to 7 M<. Intracellular (patch pipette) solutions contained (in mM): 145 Cs-methanesulfonate, 5 MgATP, 10 BAPTA, 0.2 NaGTP, and 10 mM HEPES at pH 7.2 with CsOH. Whole-cell recordings were performed with a patch-clamp amplifier (Axopatch 200, Axon Instrument, CA) after capacitance and series resistance compensation. NMDA receptor mediated currents were pharmacologically isolated by bicuculline methiodide (BMI, 10 μM, SIGMA), and 2,3-Dihydro-6-nitro-7-sulfamoyl-benzo(F)quinoxaline (NBQX; 5 μM, Tocris, St.Louis, MO). When indicated, 3-[(±)-2-carboxypiperazin-4-yl]-propyl-1-phosphonic acid, (CPP, 10 μM, Tocris) was applied. Spontaneous synaptic currents were identified using a semi-automated mini detection software (Mini Analysis Program, Jaejin Software) with threshold criteria of 10 pA (fourfold greater than the RMS noise level of 2.5 pA) and a charge transfer of 15 fC. All drugs were superfused through parallel inputs to the perfusion chamber or by means of a Y tube. For glutamate iontophoretic applications we used a micro-iontophoresis controller MVCS 02C (NPI electronics) with capacitance compensation device (Liu et al., 1999). Iontophoretic pipettes were filled with solution containing 100 mM glutamate and 10 mM glycine. Delivering currents ranged from 50 to

500 nA for 0.5 to 2 ms, depending on pipette intrinsic resistance and individual neuron response. A retain current (3–5 nA) was also delivered between every single application to avoid glutamate leakage. Currents were filtered at 1 kHz with an 8-pole low-pass Bessel filter (Frequency Devices, Haverhill, MA), digitized at 5–10 kHz using an IBM-compatible microcomputer equipped with Digidata 1200 data acquisition board (Axon Instruments, Foster City, CA) and Pclamp 8 software (Axon Instruments, Foster City, CA). Off-line data analysis, curve fitting, and figure preparation were performed with Clampfit 8 (Axon Instruments), Origin 4.1 (Microcal, Northampton, MA) and Minianalysis (Synaptosoft, Decatur GA) software. Fitting of the decay phase of currents was performed using a simplex algorithm for least squares exponential fitting routines. Decay times of averaged currents derived from fitting to double exponential equations of the form

$$I(t) = I_f \text{ X } \exp(-t/\tau_f) + I_s \text{ X } \exp(-t/\tau_s),$$

where I_f and I_s are the amplitudes of the fast and slow decay components, and τ_f and τ_s are their respective decay time constants used to fit the data. Data values are expressed as mean ± SEM unless otherwise indicated. *p* values represent the results of ANOVA with prior analysis of variance.

3. Results

3.1. Expression and functional analysis of GFP-tagged subunits in HEK293 cells

We constructed recombinants of the GFP protein tethered to the N terminus of the NR2A and NR2B subunits of the NMDA receptor. When GFP-NR2A or GFP-NR2B cDNAs were co-transfected with NR1-1a cDNA in mammalian HEK293 cells, diffuse fluorescence could be observed throughout the entire cells. Fig. 1 shows examples of cells co-transfected with GFP-NR2 and NR1-1a. Western blot analyses indicate that the increase in molecular mass in GFP-NR2 subunits (as compared to the NR2 subunit alone) is similar to the molecular mass of GFP (27 kD, Fig. 1A). Immunocytochemical staining of permeabilized HEK cells with antibodies against the NR2A subunit of NMDA receptor confirmed that GFP fluorescence corresponded to the NR2A subunit protein (Fig. 1B). Similarly, staining with NR2B subunit-selective antibodies (Fig. 1B) demonstrated that GFP-NR2B fluorescence matched NR2B subunit staining, indicating that receptors comprising NR2B and GFP tandems also contained the NR2B subunit. Both GFP-tagged subunits were located predominantly in the cytoplasmic compartment and match with the immunostaining with their cognate antibodies in permeabilized conditions. Since anti-NR2 subunit antibodies could not be used to perform surface staining, we used anti-GFP antibody to take advantage of the extracellular location of the GFP tag on the NR2 subunits. Fig. 1C illustrates GFP fluorescent HEK293 cells co-transfected with GFP-NR2A/NR1-1a or GFP-NR2B/NR1-1a and live surface immunostained by anti-GFP antibody and Cy3-conjugated secondary antibody. Surface immunostaining showed clear expression of both GFP-tagged subunits on the cell surface. The distinct fluorescent pattern between GFP and the surface anti-GFP staining indicates that the small proportion of GFP-tagged subunits on the cell surface is of too low intensity to be clearly seen with GFP fluorescence, and it is masked by the intense intracellular GFP signal. Furthermore, surface staining of GFP-NR2 transfected cells revealed the formation of subunit clusters.

We then performed electrophysiological studies on HEK293 cells transfected with constructs of NMDA receptor subunits tethered to the GFP protein. Iontophoretic glutamate applications to voltage-clamped cells (–60 mV holding potential) elicited inward currents (Fig. 1D). A study of the peak response as a function of the iontophoretic delivery charge and cell capacitance indicated that the presence of the GFP tether did not alter the NMDA current density (Fig. 1Ea). Analysis of the deactivation of currents recorded in cells transfected with wild type NR1-1a/NR2A or NR1-1a/NR2B cDNAs and cDNAs for GFP-tagged subunits revealed that the reported distinct deactivation between NR1-1a/NR2B and NR1-1a/NR2A NMDA receptor subtypes (Monyer et al., 1994; Vicini et al., 1998) is maintained in cells expressing GFP-tagged subunits (Fig. 1Eb).

These results taken together indicate that the expression of NMDA receptor subunits modified to include a fluorescent marker at their N terminus does not affect the formation of functional channels, response to agonist or deactivation kinetics.

3.2. Expression of GFP tagged subunits in neurons and live surface immunostain

Using a modification of the $CaPO_4$ precipitation technique (Chen and Okayama, 1987), we transfected primary cultures of rat hippocampal neurons. Transfected neurons were observed as early as six hours after transfection. The percent of neurons transfected was highly variable in distinct experiments but never exceeded 5% of the neurons. Cells remained transfected throughout the life of the culture (up to four weeks) but the number of fluorescent cells decreased with time along with the total cell number as defined by GFP fluorescence. Cells were successfully transfected with either GFP-NR2B or GFP-NR2A cDNAs and the percentage of transfected cells was not considerably different for the distinct plasmids. Action potential generation, occurrence of spontaneous synaptic currents and the capability to produce

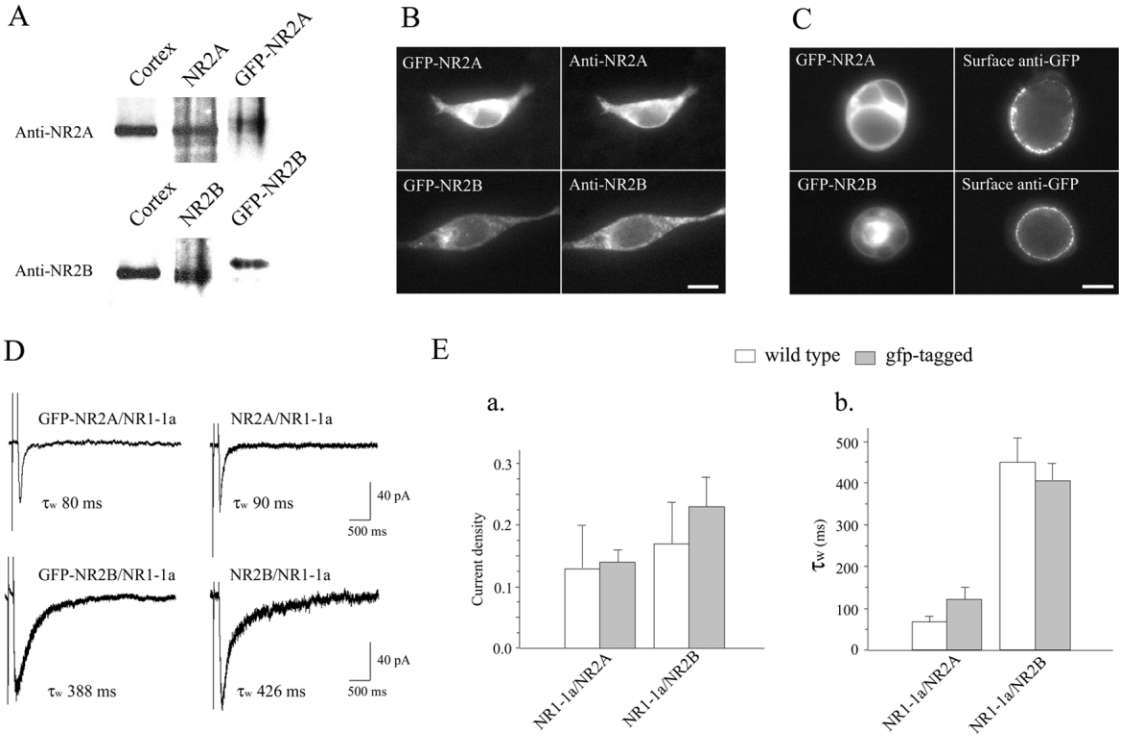

Fig. 1. Functional expression of GFP-NR2A and GFP-NR2B in HEK293 cells. (A) Membrane proteins from rat cortex and HEK293 cells transfected with cDNAs encoding for wild type and GFP-tagged NR2 subunits. GFP-NR2A and GFP-NR2B were separated on 6% SDS-PAGE and subjected to Western blot analysis probed with antibodies against NR2A and NR2B subunits, respectively. There was no other immunoreactive band detected at lower molecular mass. (B) HEK293 cells co-transfected with GFP-NR2A/NR1-1a (left top) or GFP-NR2B/NR1-1a (left bottom, GFP fluorescence) were permeabilized and immunostained by anti-NR2A- (right top) or anti-NR2B- (right bottom) specific antibodies followed by Cy3-conjugated secondary antibodies. Scale bar 10 μm. (C) GFP fluorescence of HEK293 cells co-transfected with GFP-NR2A/NR1-1a (left top) or GFP-NR2B/NR1-1a (left bottom) and then live-surface immunostained by anti-GFP antibody and Cy3-conjugated secondary antibody (right). Scale bar 10 μm.(D) Average currents evoked by at least nine iontophoretic applications of 100 mM L-glutamate for 1 ms to HEK 293 cells co-transfected with NR1-1a and GFP-NR2A (top) and with NR1-1a and GFP-NR2B (bottom) subunits. An indication of the weighted time constants (τ_w) of the double exponential decay for the current illustrated is given.(E) Summary of data measured in at least five transfected HEK cells for each distinct cDNAs combinations. (a) current density expressed as peak response (pA) per iontophoretic delivery charge (pC) and cell capacitance (pF). (b) weighted decay time constant τ_w expressed in ms.

functional synapses were not affected in transfected neurons as observed in parallel electrophysiological recordings (not shown). Two days after transfection, a diffuse and weak fluorescence was observed throughout the cells allowing the identification of dendritic branches of the transfected cell (Fig. 2) with either GFP-NR2B or GFP-NR2A cDNAs. Punctate green fluorescence was also observed on some dendrites shortly after transfection (Fig. 2). However, when compared 15 days after transfection (Fig. 2), both GFP-NR2A and GFP-NR2B transfected cells displayed clearly punctate fluorescence in most cells observed. We used a selective anti-GFP polyclonal antibody to perform surface staining of live hippocampal neurons after transfection with GFP-NR2 subunits. Surface labeling of live neurons transfected with GFP-NR2 subunits with anti-GFP primary antibody followed by Cy3-conjugated secondary antibodies revealed clear puncta that often match with the fluorescence of GFP-NR2 subunits as illustrated in Fig. 2 in the example neurons both at DIV7 and at DIV17. No staining was observed in either untransfected neurons or neurons transfected with GFP cDNA as control (Fig. 2E). At DIV17, in nine 100 μm dendritic segments from five transfected cells in three distinct experiments, we measured 49 ±7 fluorescent GFP-NR2B subunit clusters and 52 ± 9 anti-GFP Cy3-positive puncta. The extent of co-localization of GFP-NR2B with surface subunit clusters was 97 ± 4%. GFP-NR2A subunit clusters were 46 ±5 and 54 ±6, n = 10 dendrites of five cells with 87 ± 4% co-localization.

3.3. Co-localization of tagged and endogenous NMDA receptor subunits

We used immunocytochemistry with specific antibodies against the NR1, NR2A and NR2B subunits in fixed and permeabilized neurons to verify the extent of expression of GFP-tagged NR2 subunits and their co-localization with endogenous subunits in transfected neurons. As illustrated in Fig. 3, antibody staining revealed clusters in transfected neurons that were comparable to endogenous clusters in dendrites from neigh-

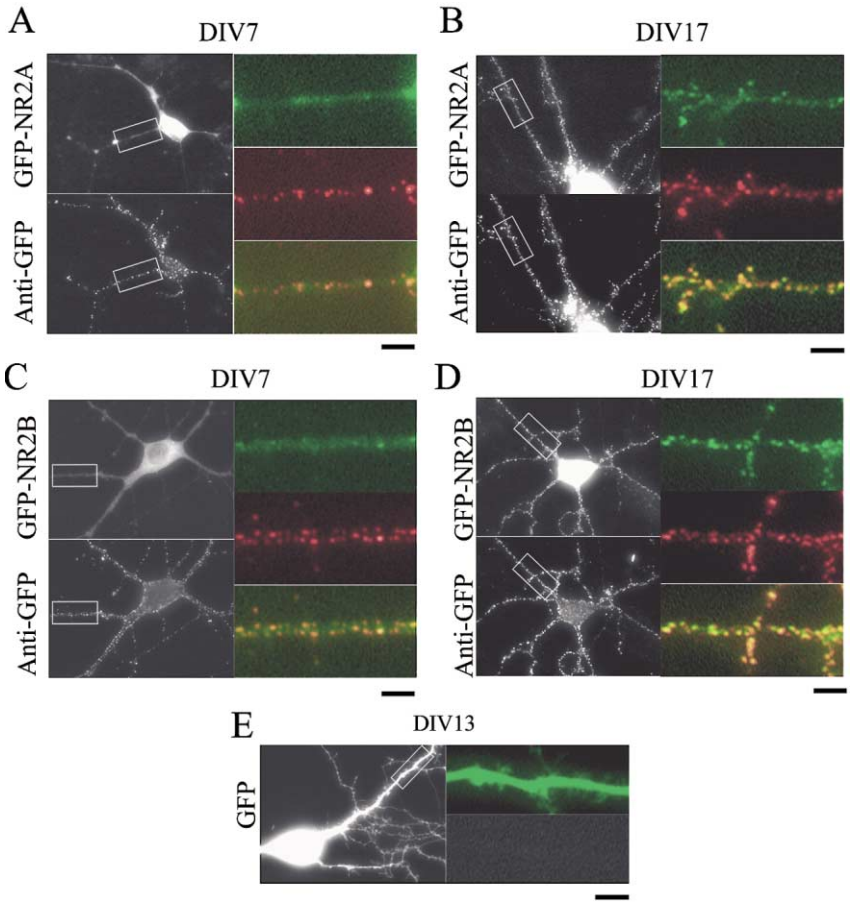

Fig. 2. Expression of GFP-NR2A and GFP-NR2B in hippocampal neurons in primary culture. Hippocampal neurons in culture were transfected at DIV5 with GFP-NR2A or GFP-NR2B, respectively, and fluorescence images were taken at DIV7 (A, C) and DIV17 (B, D). Two days after transfections (DIV7), GFP-NR2A (A) and GFP-NR2B (C) expressed with a low fluorescence intensity and in a diffused pattern with a few puncta on dendritic shafts. At DIV17, both GFP-NR2A- or GFP-NR2B- (B, D) containing clusters largely increased in number and were distributed ubiquitously along proximal and distal dendritic trees in most transfected neurons. Live hippocampal neurons expressing GFP-NR2A or GFP-NR2B subunits were also surface stained with anti-GFP and Cy3-conjugated secondary antibody at DIV7 and DIV17 (Anti-GFP). In each panel, insets show partial segments of dendrites with GFP-NR2 fluorescence (in green), anti-GFP surface stain (in red), and their merged images (overlap shown in yellow). In (E) a neuron transfected with GFP alone is illustrated together with surface staining with anti-GFP antibody. Scale bar, 15 μm and 5 μm for the insets.

boring untransfected neurons. The measurements of co-localization between GFP-tagged subunits and antibody-positive clusters were performed along individual transfected dendrites whenever possible. However, some of the unmatched clusters could have been related to the presence of non-transfected dendrites in the near vicinity of the transfected one. Figs. 3A and 3C show the co-localization of NR2A and NR2B subunit-specific antibody staining with GFP-NR2A and GFP-NR2B fluorescence. In twenty 100 μm dendritic segments from eight transfected cells in three distinct experiments using cultures at DIV12-13, we measured 58 ± 4 GFP-NR2B subunit clusters and 60 ± 4 anti-NR2B Cy3-positive puncta. The extent of co-localization of fluorescent GFP-NR2B clusters with anti-NR2B antibody-stained clusters was 96 ± 2%. Similar findings were obtained with GFP-NR2A subunit clusters (47 ± 3 and 54 ±4, n=15 dendrites of four cells, colocalization 90 ± 2%). All the GFP-tagged NR2A and NR2B fluorescent clusters were stained by corresponding antibodies. We also studied the colocalization of fluorescent GFP-NR2A and GFP-NR2B clusters and those stained by anti-NR1 subunit antibody. As illustrated in Figs. 3B and 3D, there was clear matching between GFP-NR2 subunit clusters and the presence of endogenous clusters of NR1 subunit, indicating, although not totally proving, that co-assembly of native and transfected subunits may occur together with appropriate targeting to the dendrites. In nineteen 100 μm dendritic segments from nine transfected cells in three distinct cultures at DIV12-13, we measured 46 ± 3 fluorescent GFP-NR2B subunit clusters and 49 ± 3 anti-NR1 Cy3-positive puncta. The extent of colocalization of GFP-NR2B with endogenous NR1 subunit clusters was 94 ± 2%. Similar findings were obtained with GFP-NR2A subunit clusters (59 ± 6 and 65 ± 6, n=21 dendrites of nine cells, colocalization 89

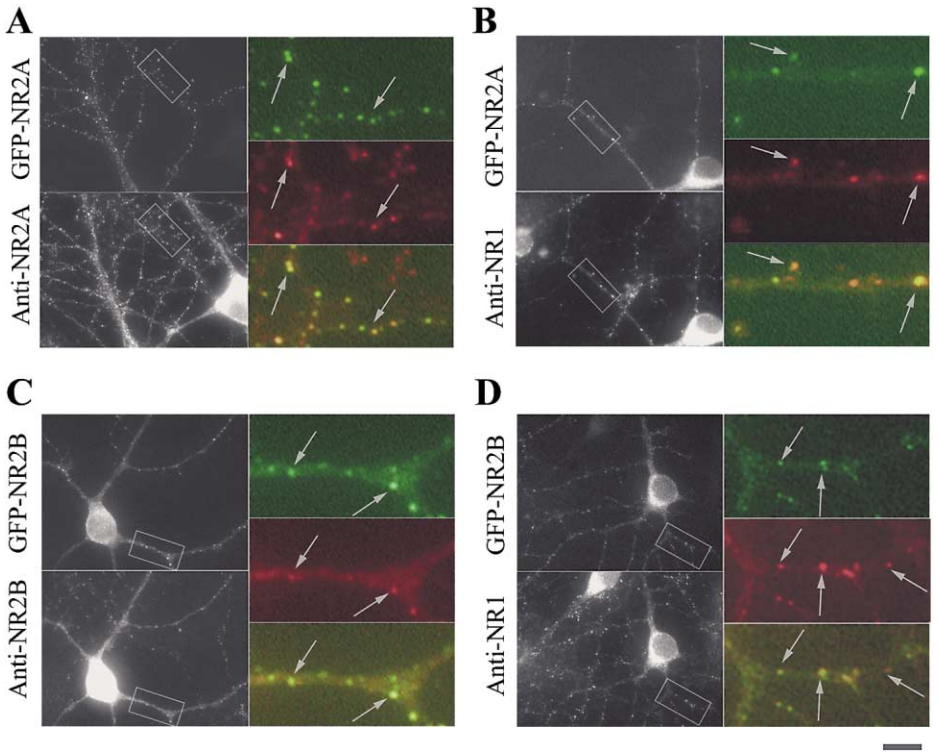

Fig. 3. Colocalization of GFP-tagged NR2 subunits with endogenous subunits in transfected hippocampal neurons in culture. GFP-NR2A- (A, B) and GFP-NR2B- (C, D) transfected neurons were fixed, permeabilized and immunostained at DIV13 with specific antibodies against NR2A (A), NR2B (C), or NR1 (B, D) followed by Cy3-conjugated secondary antibodies. Each panel shows low-power micrograph of GFP fluorescence (top left), NR subunit antibody staining (bottom left) and insets (right) with partial segments of dendrites with GFP fluorescence (in green), NR subunit antibody staining (in red), and their merged images (overlap shown in yellow). Arrows in the insets indicate example matching clusters. Non-matching clusters were also observed which mostly related to the presence of non-transfected dendrites in the field. Scale bar 15 μm and 5 μm for insets.

± 3%). Most importantly, these data are a first indication that transfected NMDA receptor subunit will likely incorporate in native NMDA receptors in hippocampal neurons. We also assessed the number of clusters of NR1, NR2A and NR2B for control neurons in matching coverslips transfected with GFP alone. In twenty 100 μm dendritic segments from eight transfected cells in three distinct experiments from cultures at DIV12-13, we measured 65 ± 1 anti-NR1 Cy3-positive clusters. Similar findings were obtained for NR2A and NR2B subunit clusters (61 ± 4 and 63 ± 1, from at least 15 dendrites of 4 cells). No statistically significant differences were observed when compared to the number of clusters per 100 μm dendritic segment in matching GFP-NR2 subunit transfected neurons.

3.4. Synaptic localization of GFP-tagged NR2 subunits

Evidence for the expression of GFP-NR2-tagged subunits at excitatory synapses in transfected neurons came from electrophysiological recordings demonstrating the occurrence of NMDA-mediated spontaneous miniature excitatory postsynaptic currents (NMDA-mEPSCs) in GFP-NR2 subunit transfected cells (Fig. 4). Whole-cell recordings were performed in cultured hippocampal neurons at DIV12-13. When neurons were voltage clamped at –60 mV, spontaneously occurring fast inward currents could be observed. These events were identified as spontaneous glutamate-mediated EPSCs resulting from the activation of alpha-amino-3-hydroxy-5-methyl-4-isoxazolepropionic acid (AMPA) receptors as they were completely abolished by NBQX (5 μM, not shown). Functional synaptic activity was recorded in all transfected neurons as AMPA receptor-mediated sEPSCs. In order to isolate NMDA-mEPSCs, experiments were performed in the presence of NBQX (5 μM), tetrodotoxin (1 μM) and BMI (20 μM) in a nominally Mg^{2+}-free solution to relieve the magnesium blockade of NMDA channels. Under these experimental conditions, an increase in the background noise and spontaneous inward currents could be observed (Fig. 4) due to activation of NMDA receptors, as further indicated by the blockade of these events by the NMDA receptors' competitive antagonist CPP (10 μM, n=5, not shown). In some cells studied, both transfected and controls, removal of magnesium and blockade of AMPA and $GABA_A$ receptors resulted in a large increase in back-

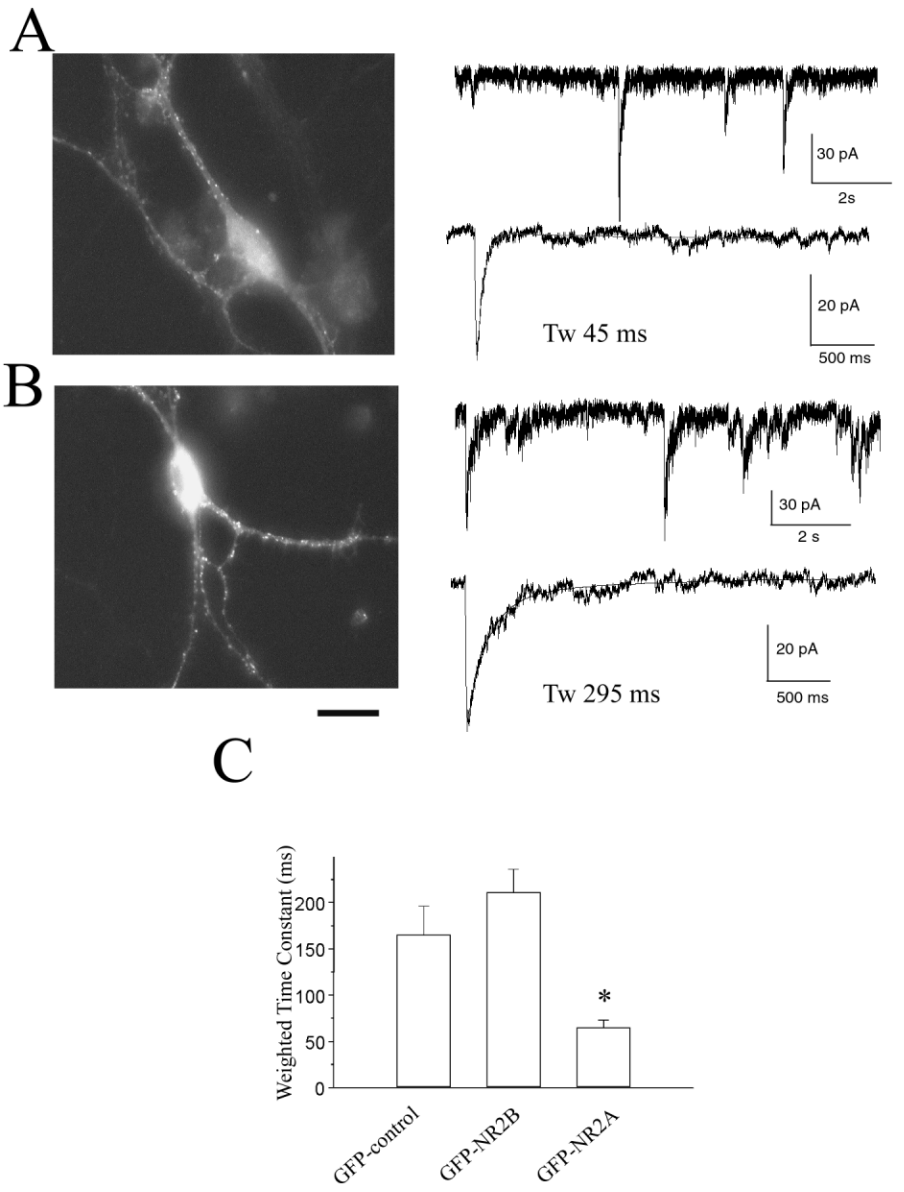

Fig. 4. NMDA-mESPCs in transfected neurons. Whole-cell recordings from hippocampal neurons in primary culture at DIV12 voltage-clamped at –60 mV in a Mg^{2+}-free solution. (A, B *left*) Fluorescent micrographs of hippocampal neurons transfected with GFP-NR2A (A) and GFP-NR2B (B) cDNAs. Scale bar 20 μm. (A,B *right*) Whole recordings of pharmacologically isolated NMDA-mEPSCs from the neuron shown to the left. The average of 15 NMDA-mESPCs is also shown with an indication of the weighted time constant of the double exponential curve used to fit the current decay time. (C) Summary of the weighted time constant of decay of NMDA-mEPSCs recorded from at least 15 neurons from three cultures transfected with GFP alone, or with GFP-NR2A or GFP-NR2B. $*$ $p<0.05$ with respect to control (ANOVA with prior analysis of variance).

ground noise with no detectable mEPSCs. In other neurons, however, pharmacologically isolated NMDA-mEPSCs were recorded as shown in the right panel from transfected neurons illustrated in the left panel of Figs. 4A and 4B. The considerable background noise precluded the estimate of amplitude and frequency of occurrence of NMDA-mEPSCs. However, exponential decay was investigated from averages of selected individual non-overlapping events and with large amplitude. In Fig. 4C, the summary data for the weighted time constant of decay are shown for NMDA-mEPSCs recorded in at least 15 neurons from three cultures transfected with GFP alone, GFP-NR2A or GFP-NR2B. As can be observed, the decay times of averaged NMDA-mEPSCs was consistently faster in GFP-NR2A-transfected cells than those of GFP transfected cells (Fig. 4C). The decay times of averaged NMDA-mEPSCs appeared slower in GFP-NR2B-transfected cells than those of GFP-transfected cells but this was not significant. The faster NMDA-mESPCs decay in GFP-NR2A-transfected neurons suggests a synaptic localization for the transfected subunit.

To further assess the colocalization of GFP-tagged NR2 subunits with a presynaptic marker, we performed

surface staining of live hippocampal neurons transfected with GFP-NR2 subunits with anti-GFP polyclonal antibody, followed by fixation and immunostaining with a selective anti-synaptophysin monoclonal antibody. As illustrated in Fig. 5 in the example neurons at DIV17, some puncta of GFP-tagged subunit surface labeling (Cy3 red) matched with the fluorescent puncta indicating synaptophysin staining (Alexa-488 green). In eleven 100 μm dendritic segments from four transfected cells in three distinct experiments, the extent of colocalization of surface GFP-NR2A subunit clusters with synaptophysin puncta measured along the transfected dendrite was 51 ± 4%. GFP-NR2B subunit clusters/synaptophysin puncta colocalization was 49 ± 6%. (n = 16 dendrites of four cells).

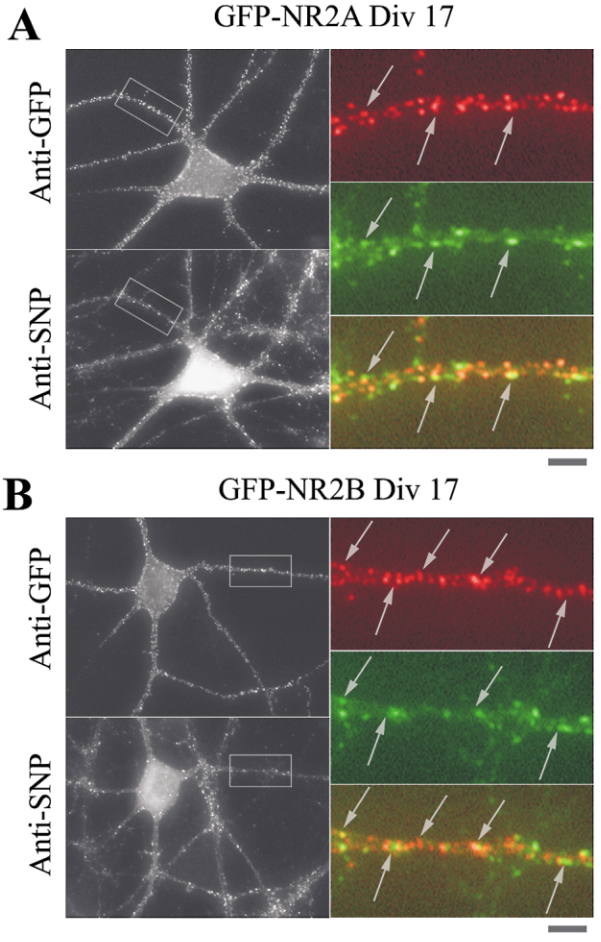

Fig. 5. Colocalization of surface GPF-NR2 clusters with synaptophysin. GFP-NR2A- (A) and GFP-NR2B- (B) transfected neurons at DIV17 were surface stained live with anti-GFP primary and Cy3-conjugated secondary antibodies (Anti-GFP, top left), followed by fixation, permeabilization and immunostain with anti-synaptophysin primary and Alexa-488 secondary antibodies (Anti-SNP, bottom left). Insets (right) with partial segments of dendrites with anti-GFP-Cy3 fluorescence (in red), synaptophysin subunit antibody staining (in green), and their merged images (overlap shown in yellow). Arrows in the insets indicate matching examples. Scale bar 15 μm and 5 μm for insets.

3.5. Localization of GFP-NR2 subunits in dendritic structures

Using co-transfection with a construct expressing actin tagged with cyan fluorescent protein (CFP-actin), we were able to observe detailed dendritic anatomy in cells co-transfected with this plasmid and the GFP-NR2 constructs. As it can be seen in Fig. 6, most hippocampal cells at DIV8 had long filopodia. In time-lapse studies these filopodia were highly motile (not shown). In contrast, at DIV16, most cells displayed dendrites covered with well-defined spines. This developmental transformation in dendrites from filopodia to spines at the time of synaptogenesis has been extensively studied previously (Fischer et al., 1998; Jontes and Smith, 2000; Matus 2000; Segal and Andersen, 2000 for review). In thirty five 100 μm dendritic segments from 22 CFP-actin-transfected cells in four distinct experiments at DIV7, we counted 43 ± 3 filopodia and 3 ± 1 dendritic spines per segment. In forty two 100 μm dendritic segments from 19 transfected cells in four distinct experiments at DIV16, we counted 4 ± 1 filopodia and 61 ± 2 dendritic spines per segment. In Figs. 7A and 7B, the relative density of filopodia and spines is compared for neurons at DIV7 and DIV16 transfected with GFP-NR2A and GFP-NR2B, respectively. In these cells, we also illustrate the distribution of the NMDA receptor subunits seen after transfection of the GFP-NR2 constructs and live surface labeling with anti GFP antibody and Cy3-conjugated secondary antibody. The weak GFP fluorescence of tagged NR2 subunits did not bleed through the CFP band pass cube with the exposures used to photograph the bright CFP-actin fluorescence. As can be seen, most NMDAR clusters in cells at DIV7 were localized to the base of the filopodia rather than on their tips. In contrast, at DIV16, all Cy3-positive puncta corresponding to the surface expression of GFP-NR2 subunits were clearly localized to dendritic spines and shafts. This was true for both NR2A and NR2B constructs. In Figs. 7C and 7D the percent of GFP-tagged subunits localized to filopodia versus dendritic shafts in several 100 μm dendritic segments is reported for both GFP-NR2A and GFP-NR2B-transfected neurons at DIV7 and DIV16. In cells at DIV7, anti-GFP surface staining revealed a larger number of clusters in transfected cells than visualized by GFP fluorescence (compare Fig. 2 with Fig. 6).

4. Discussion

Our study investigated NR2A and NR2B subunits N-terminally fused with GFP in transfected HEK293 cells and hippocampal neurons in culture. GFP-NR2A and GFP-NR2B subunits form functional NMDA channels and produce observable fluorescence when co-transfected with untagged NR1-1a subunit partner in HEK293

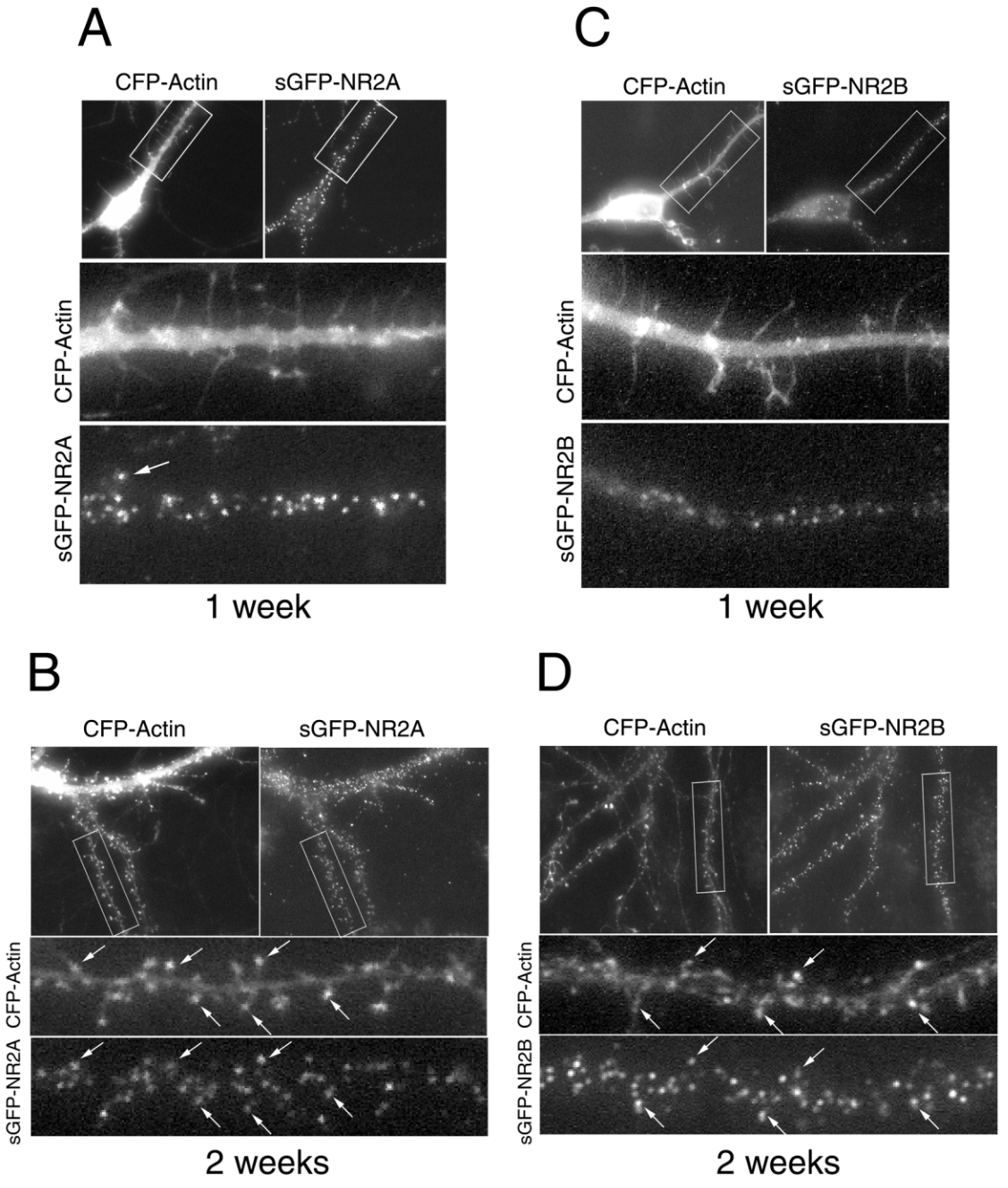

Fig. 6. Anatomical location of NR2 clusters. Live hippocampal neurons expressing CFP-actin and GFP-NR2A or GFP-NR2B subunits were surface stained with anti-GFP and Cy3-conjugated secondary antibody at DIV8 and DIV16 (sGFP-NR2). (A, B) A comparison of GFP-tagged NR2A (A) and NR2B (B) subunit clusters in neurons at DIV7. The distribution of NMDA receptor clusters is in the dendritic shafts and sometimes at the base of the filopodia. Partial dendrites in dashed rectangles were amplified and showed on the bottom for each image. Scale bar, 20 μm and 5 μm for the insets. The arrow in the insets indicates a cluster on a filopodia. (C, D) A comparison of GFP-tagged NR2A (C) and NR2B (D) subunit clusters in neurons at DIV16. Receptor clusters are located both on spines and dendritic shafts. Partial dendrites in dashed rectangles were amplified and showed on the bottom for each image. Scale bar, 20 μm and 5 μm for the insets. The arrows in the insets indicate examples of clusters on dendritic spines.

cells. Surface staining with anti-GFP antibody illustrated that only a portion of the tagged subunits are expressed on cell surfaces and form aggregates of fluorescent proteins. Electrophysiological recordings from transfected HEK293 cells independently confirmed the surface expression of functional NMDA channels comprising GFP-tagged subunits. These channels had similar deactivation kinetics to untagged NMDA receptor subtypes (Monyer et al., 1994; Vicini et al., 1998).

Expression of GFP-NR2A and GFP-NR2B subunits in transfected hippocampal neurons was successful as indicated by the mostly diffuse fluorescence and pres-

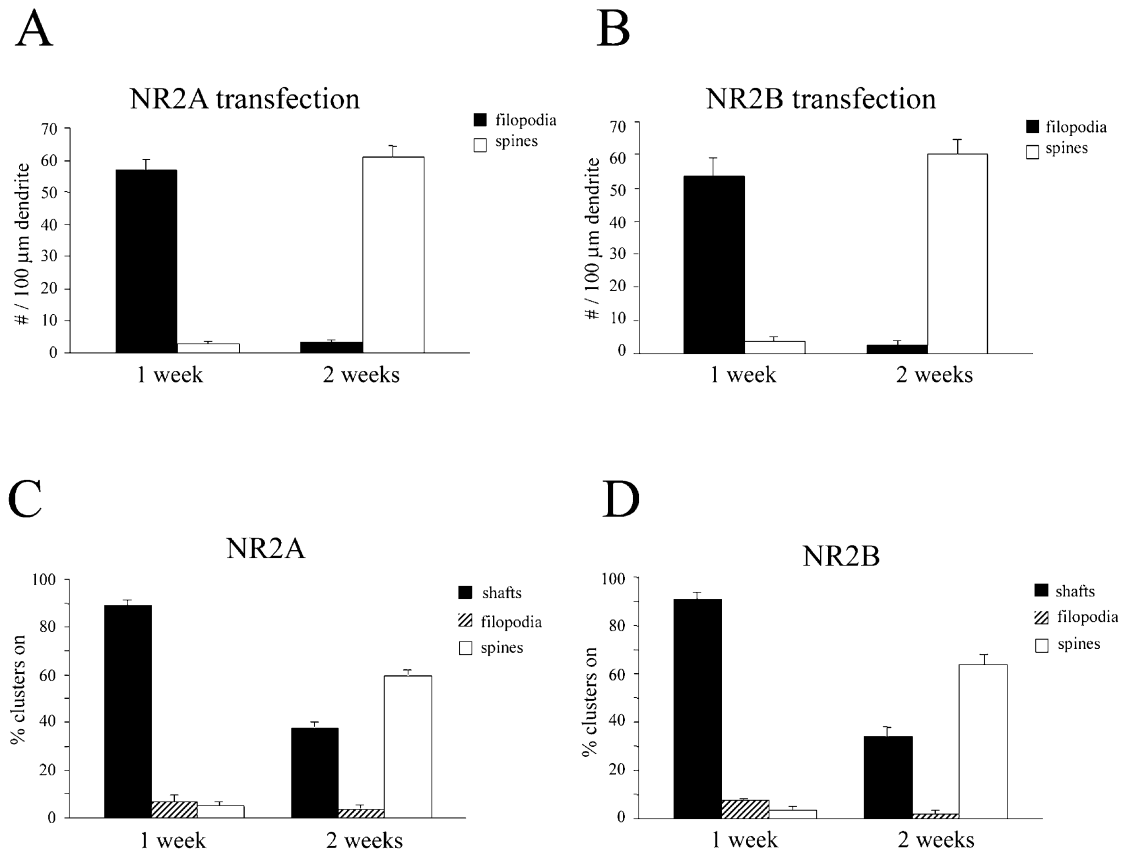

Fig. 7. Summary of results on the anatomical location of NR2 clusters. (A, B) Summary of results of the study of the relative number of filopodia and spines on dendrites of transfected neurons expressing CFP-actin at 7–8 DIV (1 week) and 15–16 DIV (2 weeks) when co-transfected with GFP-NR2A (A) or GFP-NR2B (B) subunits and surface stained with anti-GFP and Cy3-conjugated secondary antibody. (C, D) Summary of the density of NR2 subunit receptor clusters on filopodia as compared to dendritic shafts and spines on dendrites of transfected neurons expressing CFP-actin at 7–8 DIV (1 week) and 14–15 DIV (2 weeks) when co-transfected with GFP-NR2A (C) or GFP-NR2B (D) subunits and surface stained with anti-GFP and Cy3-conjugated secondary antibody.

ence of a few individual clusters. GFP-NR2B subunit clusters were seen early after transfection while GFP-NR2A subunit expression was weaker but increased with development in vitro. As development progresses, more defined clusters and less diffuse fluorescence were observed along the dendritic processes of neurons transfected with either GFP-NR2A or GFP-NR2B. Well-defined clusters several days after transfection have been reported in hippocampal neurons transfected with C-terminal fused NR1-GFP constructs (Crump et al., 2001). However, when we performed surface staining in live neurons with anti-GFP antibody taking advantage of the extracellular location of the GFP tag, the clear formation of clusters on the cell surface for both NR2A and NR2B subunits could be observed at any age investigated. Quantitation of the numbers of GFP clusters and clusters labeled by anti-GFP antibody indicate that 15 days after transfection the observable GFP clusters are indeed expressed on the cell surface. This suggests that GFP clusters can be used to perform dynamic studies of NMDA receptor in living neurons at that age. However, in cells early after transfection as well as with low expression, anti-GFP surface staining revealed a larger number of clusters in transfected cells than visualized by GFP fluorescence. What is the reason for this discrepancy? It is likely that a small proportion of tagged-subunit containing receptors in a single cluster makes it impossible for these clusters to be seen clearly by GFP fluorescence, but they can be revealed by the amplification of the primary/secondary antibody staining. It is possible that the labeling by live surface staining with anti-GFP antibody is a more sensitive indicator of the surface expression of tagged subunits. However, live surface staining with antibodies also has limitations, most notably in the capability to follow receptor subunit dynamics in time. For these studies, the best approach will therefore have to include assessment of tagged subunit clusters with both GFP fluorescence and live surface staining.

Immunocytochemical staining after permeabilization using specific antibodies against NR2A and NR2B subunits, respectively, showed that the clusters of tagged subunits match quite well with endogenous clusters for both NR2A and NR2B subunits in hippocampal neurons

several days after transfection. These results illustrate that most of the endogenous receptors include GFP tagged subunits. Thus, this supports the use of GFP-tagged subunits as an indication of native subunit clusters. GFP-NR2A and GFP-NR2B clusters co-localize with endogenous NR1 clusters as indicated from NR1-specific antibody staining in permeabilized neurons. Therefore, we can speculate that tagged subunit clusters include the NR1 subunit, an essential component to functional channel formation. Furthermore, the fact that all tagged NR2 subunit clusters had an NR1 counterpart indicates that the transfection did not induce the formation of isolated tagged subunit clusters. Last, the similar density of clusters of NR1, NR2A and NR2B subunits in transfected and untransfected neurons suggests that transfection procedures did not induce the formation of additional NMDA receptor complexes.

Whole-cell recordings from transfected neurons suggested the insertion of GFP-tagged subunits into the synaptic receptor pool as indicated by the fast weighted time constant in GFP-NR2A-transfected cells. At the developmental stage of the neurons in which we performed electrophysiology recordings, the NR2B subunit is predominant in the synaptic NMDA receptors. This could explain the lack of significant alterations in kinetics of NMDA mEPSCs in GFP-NR2B-transfected neurons. An alternative explanation is that the GFP tag prevents the surface expression of the NR2B subunit. To gain insights between these possibilities we performed surface immunostaining in live cells of GFP-tagged NR2 subunits followed by permeabilization and staining with anti-synaptophysin antibody. The results revealed that approximately half of both GFP-tagged NR2 subunits were clearly juxtaposed to presynaptic boutons indicating the likely synaptic expression of a good portion of both GFP-tagged subunits.

Taking advantage of our labeling technique to visualize NR2A and NR2B subunits in living neurons, we investigated their occurrence with respect to the reported changes in the dendritic dynamics in synaptogenesis. In these studies, a progressive decline in the number of filopodia and increase in stubby and mushroom spines has been observed as excitatory synapses form both in vitro (Dailey and Smith., 1996; Ziv and Smith, 1996; Fischer et al., 1998; 2000; Matus, 2000; Segal and Andersen, 2000; Korkotian and Segal, 2001; Okabe et al., 2001) and in vivo (Fiala et al., 1998; Maletic-Savatic et al., 1999; Lendvai et al., 2000). Our results showed that both GFP-NR2A and GFP-NR2B clusters are found mostly in dendritic shaft, sometimes at the base of filopodia and rarely on the tip of filopodia in the first week after plating, a time when synaptogenesis has been demonstrated to occur with staining against synaptophysin and functional assessment of synaptic formation in hippocampal culture (Renger et al., 2001). In contrast, in the second week after plating, after synapses are formed, the dendritic trees of hippocampal neurons are covered with spines. At this time, we showed that both NR2A and NR2B subunit clusters are found in the many spine heads. However, a large number of subunit clusters are still seen on the dendritic shaft. These results are reminiscent of those found with electron microscopy (Fiala et al., 1998) and with GFP-tagged PSD-95 (Okabe et al., 2001). Although it has been shown that spine formation occurs in neuronal culture from NR1subunit knockout mice (Okabe et al., 1998), it is possible that different NMDA receptor subunits play a distinct role in the temporal sequence from the filopodia retraction to the formation of the synapses on the spine head. Our results show the possibility of studying NMDA receptor clusters in neurons in parallel with the observation of dendritic dynamics and synapse formation.

Acknowledgements

Supported by NIH grants RO1 MH58946 RO1 NS28709, KO2 MH01680, the Bundy Foundation and the Hereditary Disease Foundation Lieberman Award to BV.

References

Connor, J.X., Boileau, A.J., Czajkowski, C., 1998. A $GABA_A$ receptor $\alpha 1$ subunit tagged with green fluorescent protein requires a beta subunit for functional surface expression. Journal of Biological Chemistry 273, 28906–28911.

Crump, F.T., Dillman, K.S., Craig, A.M., 2001. cAMP-dependent protein kinase mediates activity-regulated synaptic targeting of NMDA receptors. Journal of Neuroscience 21, 5079–5088.

Cubitt, A.B., Heim, R., Adams, S.R., Boyd, A.E., Gross, L.A., Tsien, R.Y., 1995. Understanding improving and using green fluorescent proteins. Trends in Biochemical Science 20, 448–455.

Cubitt, A.B., Woollenweber, L.A., Heim, R., 1999. Understanding structure–function relationships in the Aequorea victoria green fluorescent protein. Methods in Cell Biology 58, 19–30.

Cull-Candy, S., Brickley, S., Farrant, M., 2001. NMDA receptor subunits: diversity development and disease. Curr Op Neurobiol 16, 327–335.

Dailey, M.E., Smith, S.J., 1996. The dynamics of dendritic structure in developing hippocampal slices. Journal of Neuroscience 16, 2983–2994.

David-Watine, B., Shorte, S.L., Fucile, S., de Saint Jan, D., Korn, H., Bregestovski, D.P., 1999. Functional integrity of green fluorescent protein conjugated glycine receptor channels. Neuropharmacology 38, 785–792.

Daw, N.W., Stein, P.S., Fox, K., 1993. The role of NMDA receptors in information processing. Annual Review of Neuroscience 16, 207–222.

Dingledine, R., Borges, K., Bowie, D., Traynelis, S.F., 1999. The glutamate receptor ion channels. Pharmacological Review 51, 7–61.

Fiala, J.C., Feinberg, M., Popov, V., Harris, K.M., 1998. Synaptogenesis via dendritic filopodia in developing hippocampal area CA1. Journal of Neuroscience 18, 8900–8911.

Fischer, M., Kaech, S., Knutti, D., Matus, A., 1998. Rapid actin-based plasticity in dendritic spines. Neuron 20, 847–854.

Fischer, M., Kaech, S., Wagner, U., Brinkhaus, H., Matus, A., 2000. Glutamate receptors regulate actin-based plasticity in dendritic spines. Nature Neuroscience 3, 887–894.

Fox, K., Henley, J., Isaac, J., 1999. Experience-dependent development of NMDA receptor transmission. Nature Neuroscience 2, 297–299.

Jontes, J.D., Smith, S.J., 2000. Filopodia; spines and the generation of synaptic diversity. Neuron 27, 11–14.

Korkotian, E., Segal, M., 2001. Regulation of dendritic spine motility in cultured hippocampal neurons. Journal of Neuroscience 21, 6115–6124.

Lendvai, B., Stern, E.A., Chen, B., Svoboda, K., 2000. Experience-dependent plasticity of dendritic spines in the developing rat barrel cortex in vivo. Nature 404, 876–881.

Li, J.H., Wang, Y.H., Wolfe, B.B., Krueger, K.E., Corsi, L., Stocca, G., 1998. Developmental changes in localization of NMDA receptor subunits in primary cultures of cortical neurons. The European Journal of Neuroscience 10, 1704–1715.

Liu, G., Choi, S., Tsien, R.W., 1999. Variability of neurotransmitter concentration and non-saturation of postsynaptic AMPA receptors at synapses in hippocampal cultures and slices. Neuron 22, 395–409.

Luo, J., Wang, Y.H., Yasuda, R.P., Dunah, A., Wolfe, B.B., 1997. The majority of N-Methyl-D-Aspartate receptor complexes in adult rat cerebral cortex contain at least three different subunits. Molecular Pharmacology 51, 79–86.

Maletic-Savatic, M., Malinow, R., Svoboda, K., 1999. Rapid dendritic morphogenesis in CA1 hippocampal dendrites induced by synaptic activity. Science 283, 1860–1861.

Marshall, J., Molloy, R., Moss, G.W., Howe, G.R., Hughes, T.E., 1995. The jellyfish green fluorescent protein: a new tool for studying ion channel expression and function. Neuron 14, 211–215.

Matus, A., 2000. Actin-based plasticity in dendritic spines. Science 290, 754–758.

Monyer, H., Burnashev, H., Laurie, D.J., Sakmann, B., Seeburg, P.H., 1994. Developmental and regional expression in the rat brain and functional properties of the four NMDA receptors. Neuron 12, 529–540.

Okabe, S., Vicario-Abejon, C., Segal, M., McKay, R.D., 1998. Survival and synaptogenesis of hippocampal neurons without NMDA receptor function in culture. The European Journal of Neuroscience 10, 2192–2198.

Okabe, S., Miwa, A., Okado, H., 2001. Spine formation and correlated assembly of presynaptic and postsynaptic molecules. Journal of Neuroscience 21, 6105–6114.

Renger, J.J., Egles, C., Liu, G., 2001. A developmental switch in neurotransmitter flux enhances synaptic efficacy by affecting AMPA receptor activation. Neuron 29, 469–484.

Segal, M., Andersen, P., 2000. Dendritic spines shaped by synaptic activity. Current Opinion in Neurobiology 10, 582–586.

Sheetz, A.J., Constantine-Paton, M., 1994. Modulation of NMDA receptor function: implication for vertebrate neural development. FASEB Journal 8, 745–752.

Shi, S.H., Hayashi, Y., Petralia, R.S., Zaman, S.H., Wenthold, R.J., Svoboda, K., 1999. Rapid spine delivery and redistribution of AMPA receptors after synaptic NMDA receptor activation. Science 284, 1811–1816.

Vicini, S., Wang, J.F., Li, J.H., Zhu, W.J., Wang, Y.H., Luo, J.H., 1998. Functional and pharmacological differences between recombinant N-methyl-D-aspartate receptors. Journal of Neurophysiology 79, 555–566.

Ziv, N.E., Smith, S.J., 1996. Evidence for a role of dendritic filopodia in synaptogenesis and spine formation. Neuron 17, 91–102.